



Why large Flakes? Later Acheulian handaxe manufacture at Amanzi Springs, Area 2 (Eastern Cape, South Africa)

Coen G. Wilson^{a,*}, Matthew V. Caruana^b, Alexander F. Blackwood^{a,c,d}, Lee J. Arnold^e, Andy I. R. Herries^{a,b}

^a Palaeoscience, Department of Archaeology and History, La Trobe University, Melbourne Campus, Bundoora 3086, VIC, Australia

^b The Palaeo-Research Institute, University of Johannesburg, P.O. Box 524, Auckland Park 2006, Gauteng, South Africa

^c Human Evolution Research Institute (HERI), University of Cape Town, Western Cape, South Africa

^d Human Palaeosystems Group, Max Planck Institute of Geoanthropology, Jena, Germany

^e Environment Institute, and Institute for Photonics and Advanced Sensing (IPAS), School of Physical, Chemistry and Earth Sciences, University of Adelaide, Adelaide, South Australia 5005, Australia

ARTICLE INFO

Keywords:

Amanzi Springs
Handaxes
Later Acheulian
Large Flakes
3D Geometric Morphometric
South Africa

ABSTRACT

Recent studies have identified differences in handaxe reduction strategies within the Acheulian assemblages from Amanzi Springs, with operational sequences that involve a variety of giant core methods to produce large flake blanks, as well as being made directly on cobbles. Despite these different blank selection patterns, there is a general standardisation in the final morphology of handaxes from Area 2 (~530 – <408 ka). This study uses three-dimensional geometric morphometric, descriptive statistics and diacritical analyses to explore large flake usage at the site, and its implications in handaxe morphology and manufacture. Our results demonstrate that Amanzi knappers used large flake blanks with standardised characteristics and morphologies to shortcut challenging technical aspects of handaxe production. Despite previous descriptions of handaxes being large and unstandardised in appearance, Middle Pleistocene knappers at Amanzi Springs were able to anticipate challenges of the locally available raw materials by producing a range of large flake blank morphologies to overcome knapping mishaps.

1. Introduction

The production of large flakes (>100 mm) as blanks for large cutting tools (LCT) is a technological hallmark of the Acheulian technocomplex (Sharon, 2007, 2010). A variety of giant core reduction methods has been documented at Acheulian sites, which are in some cases specifically predetermined for handaxe or cleaver shaping (Texier and Roche, 1995; Petraglia et al., 1999; Madsen and Goren-Inbar, 2004; Sharon and Beaumont, 2006; Sharon, 2007, 2009, 2010, 2011, 2019; Shipton et al., 2009; McNabb and Beaumont, 2011; Gallotti and Mussi, 2017; Herzlinger et al., 2017b; Li et al., 2017). Despite variability in giant core reduction strategies and raw materials, it is argued that LCTs produced using large flake (>10 cm in length) blanks appear to be more standardised in form (Sharon, 2007, 2008, 2009, 2010; Sharon et al., 2011), when compared to handaxes manufactured on cobbles or tabular clasts. Large flake production therefore implies that Acheulian knappers understood how to attain blanks with the desired geometric features that

were optimal for shaping LCTs. Sharon (2007, 2009, 2010) further highlighted that morphological variability in LCTs is directly related to blank selection. In addition, large flaking methods allow knappers to shortcut aspects of the LCT shaping process, such as complex thinning procedures, while also maintaining an extended cutting edge (Jones, 1994; Goren-Inbar and Saragusti, 1996; Madsen and Goren-Inbar, 2004; Winton, 2005; Sharon, 2007, 2010; Shipton et al., 2009; Wynn and Gowlett, 2018).

One site that has the potential to provide important information on this debate is Amanzi Springs, located ~ 40 km north of Gqeberha (formerly Port Elizabeth) in the Eastern Cape Province of South Africa (Fig. 1A). The site has yielded impressive finds of preserved wood and organic material, along with an abundance of diagnostic Acheulian material in stratified settings from two spring eyes that were excavated by Ray Inskeep and Hilary Deacon in the 1960's (Inskeep, 1965; Deacon, 1970). Recent studies have identified differences in handaxe reduction strategies within the Acheulian assemblages from the Area 1 (~404 –

* Corresponding author.

E-mail address: coenwilson1@gmail.com (C.G. Wilson).

<https://doi.org/10.1016/j.jasrep.2024.104393>

Received 24 June 2023; Received in revised form 2 January 2024; Accepted 13 January 2024

Available online 30 January 2024

2352-409X/© 2024 The Author(s). Published by Elsevier Ltd. This is an open access article under the CC BY license (<http://creativecommons.org/licenses/by/4.0/>).

390 ka) and Area 2 (~530 – <408 ka) spring eyes at Amanzi Springs, which included a variety of large flaking methods (including the *entame* and slab slice types), along with direct bifacial reduction of cobbles (Herries et al., 2022; Caruana et al., 2023). In contrast, at Area 2 there is an increase in large flake blanks in the younger (<481 or < 408 ka) Surface 1 assemblage compared to the older Surfaces 2 and 3 handaxes (~530 – 481 ka) (Caruana et al., 2023). These patterns suggest temporal differences in the use of large flake blanks to manufacture handaxes at the site, and here we investigate its potential advantages.

Previous research has focused on the causes of variation in handaxe forms at Amanzi Springs, which was initially described as “heavy and unstandardized” (Deacon, 1970: 98). Analyses of handaxe production at Amanzi Springs has highlighted considerable morphological variation across different stratigraphic layers and spring eyes (Caruana, 2021, Caruana et al., 2022, Caruana et al., 2023). Herries et al. (2022) demonstrated that the Area 1 handaxe assemblage does not conform to expected typological or technological trends of the later Acheulian period. More recently, our analyses have demonstrated that the

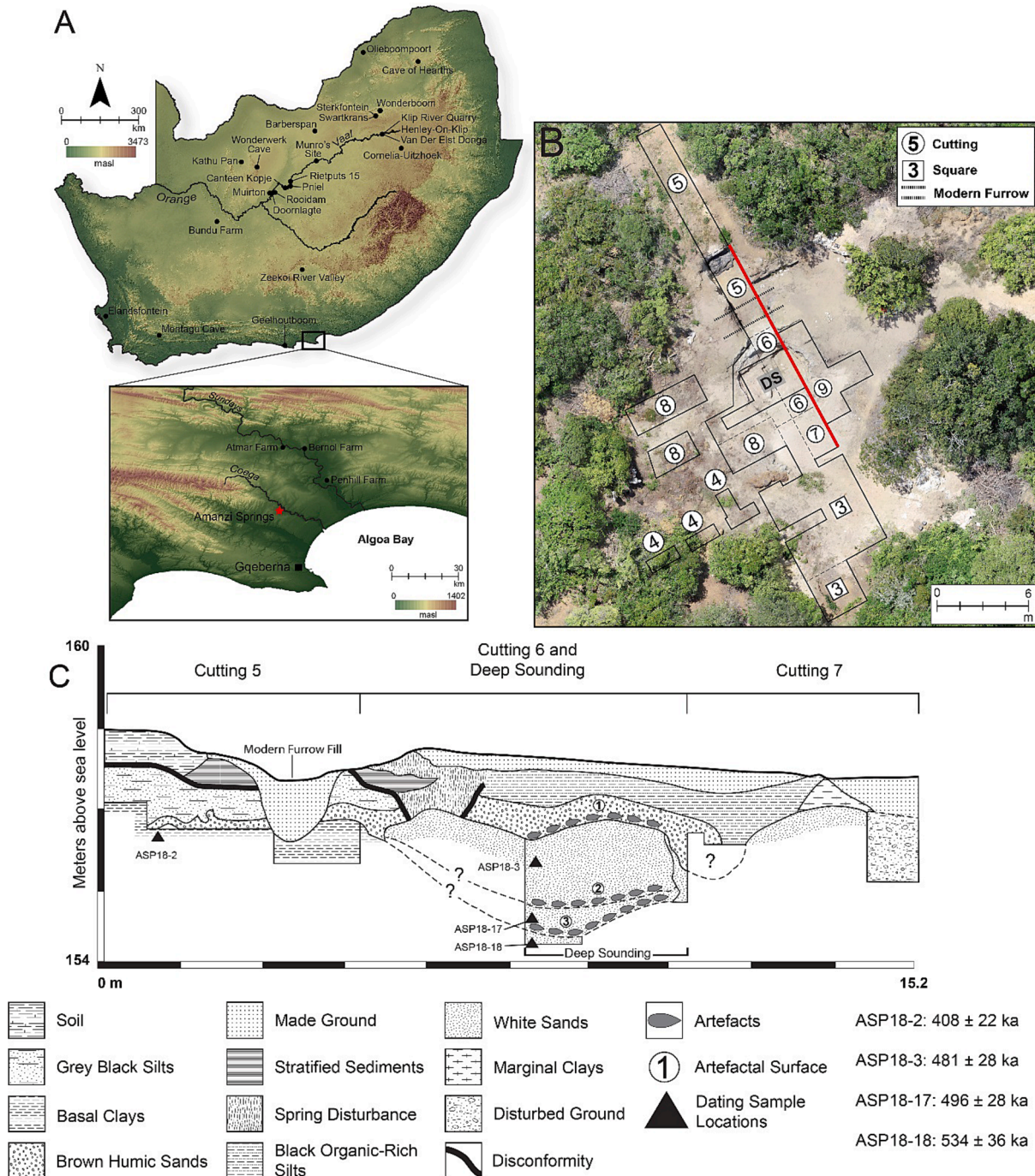


Fig. 1. A) Map of South Africa with documented Acheulian sites. Inlay of the Algoa Bay region (Eastern Cape Province), which shows the location of Amanzi Springs. B) Map of Deacon's (1970) excavation grid in Area 2, red line represents section of stratigraphy shown in (C); Adapted from Caruana et al., 2023). C) The stratigraphy of Area 2 East Wall (redrawn from Deacon, 1970) with approximate locations of the luminescence dating samples taken in Cutting 5, Surface 1 and Deep Sounding excavations (black triangles). The luminescence ages shown in the legend have been calculated from the weighted mean of the replicate TT-OSL and pIR-IR ages for each sample, and are presented with their combined 1σ uncertainty ranges (Adapted from Caruana et al., 2023).

interplay between raw material quality and knapping mistakes during the manufacturing process often led to early discard during primary shaping phases (Caruana and Herries, 2020, 2021; Caruana, 2021; Caruana et al., 2022, 2023). Thus, their morphology does not represent the extent of technological knapping skill typical of later Acheulian toolmakers, but rather tools that were discarded before they reached the finishing phases of the reduction sequence. In addition, the site is hypothesized to represent a raw material procurement and LCT workshop site (Keller, 1973, Sharon, 2007, Caruana & Herries, 2020, 2021, Caruana et al., 2023). This has been inferred by the LCTs representing different stages of reduction with several un-finished or in the rough-out stage of manufacture (Keller, 1973, Sharon, 2007, Caruana and Herries, 2020).

Given the observed increase in large flake blank use through time in the Area 2 Deep Sounding assemblages, the aim of this study is to compare technological and morphological variation in large flake versus cobble-reduced handaxes from Deacon's (1970) excavated assemblages from Surfaces 2/3 (~530 – 481 ka), Surface 1 (<481 or < 408 ka) and Cutting 5 (<408 ka) (Caruana et al., 2022, 2023). Our goal is to investigate whether large flake blanks provided any benefits in shortcutting handaxe reduction sequences, specifically to avoid shaping phases that were prone to knapping mishaps (i.e., the development of step and hinge fractures and thick bifacial edges) (Caruana and Herries, 2021; Caruana et al., 2022). To do so, we contrast morphological and technological variability between handaxes made on large flakes produced through different giant core methods. We present a series of three dimensional geometric morphometric, descriptive statistical, and diacritical analyses to explore large flake usage at the site, and its role in handaxe morphology and manufacture. We then use these data to explore the behavioural and cognitive implications of diachronic changes in large flaking techniques and blank use.

1.1. A brief review of Acheulian large flaking methods

A high proportion of LCTs were made on large flake blanks, which are common at Acheulian sites younger than ~ 1 Ma, and which we informally refer to as the 'later' Acheulian period (McNabb et al., 2004, McNabb, 2009, Archer and Braun, 2010; Shipton, 2011; Shipton et al., 2014; de la Torre et al., 2014; Sharon, 2007, 2010; Gallotti et al., 2014; Gallotti and Mussi, 2017; Goren-Inbar et al., 2018; Caruana et al., 2023). Strategies for shaping LCTs made using large flake blanks primarily focused on the modification of the dorsal surface, with the ventral side being largely left untouched except for the systematic trimming of percussion bulbs (Sharon, 2010). Despite raw material variation, LCT manufacturing processes on large flake blanks were fairly uniform (Sharon, 2008). Sharon (2007, 2008) further argued that increased use of large flaking methods in LCT manufacturing was coupled with increased mobility patterns in later Acheulian hominin populations (cf., Potts et al., 1999; Hallos, 2005; Archer and Braun, 2010; Preysler et al., 2018; Presnyakova et al., 2018). While the later Acheulian is associated with increased technical demands related to giant core reduction methods, the ability to predetermine blank morphologies lessened the dependence of Acheulian toolmakers on river cobble beds. Once obtained, blanks could be transported over longer distances away from raw material sources, which is further corroborated by fragmentation in LCT reduction chains at Middle Pleistocene sites (Hallos, 2005; Presnyakova et al., 2018; Caruana, 2022).

By ~ 1 Ma years or slightly before, several specialised giant core reduction methods appear at Acheulian sites, including Victoria West (Sharon and Beaumont, 2006; McNabb and Beaumont, 2011; Li et al., 2017), Kombewa (Owens, 1938; Texier and Roche, 1995; Schick and Clark, 2003), *entame* (i.e., cobble opening; Sharon, 2011; Gallotti et al., 2021, 2023), Tabelbala-Tachenghit (Tixier, 1956; Alimen, 1978; Sharon, 2009), slab-slice (Paddayya, 1977, 1982; Goren-Inbar et al., 2018), Levallois (Tyron et al., 2005; Shipton, 2022) and a variety of other unifacial and bifacial methods (Madsen and Goren-Inbar, 2004;

Sharon, 2007). At the later Acheulian site of Kalambo Falls (~500 – ~300 ka; Duller et al., 2015; Barham et al., 2023), large flake blanks were produced through prepared discoidal cores, where the circumference of a boulder was bifacially flaked whilst maintaining adequate edge angles (Toth, 2001). Similar methods were adopted by Acheulian knappers at Gesher Benot Ya' aqov (~780 ka; Goren-Inbar et al., 2018), where large bifacially worked basalt cores were knapped using alternate flaking sequences (Madsen and Goren-Inbar, 2004). Madsen and Goren-Inbar (2004, p.45) note that greater control can be obtained during the knapping processes by preparing and striking a plain platform in between facets to control the morphology of the detached blanks. At Isampur Quarry (India) (~1.2 Ma; Paddayya et al., 2002), cleaver flakes were obtained from thick limestone slabs, prepared by centripetal removals orientated at right angles to the bedding plane, which established the necessary detachment angles and platforms (Petraglia et al., 2005; Shipton et al., 2009).

In eastern Africa, the use of the Kombewa method for producing standardised blanks becomes common after ~ 800 ka (Owen, 1938; Texier and Roche, 1995; Schick and Clark, 2003; Sharon, 2009; Gallotti and Mussi, 2017). A large flake is first removed from a boulder or cobble, which then serves as the core for the detachment of a Kombewa flake struck from the ventral face (Sharon, 2009). The resulting blanks have an equally distributed volume, with two convex faces connected by an extended cutting edge, which requires limited shaping to produce an LCT (Sharon, 2009; Gallotti and Mussi, 2017). In southern Africa, the Victoria West method has been documented at several sites along the Vaal River by around ~ 1 Ma (Sharon and Beaumont, 2006; McNabb and Beaumont, 2011; Leader, 2014; Li et al., 2017). These cores were hierarchically organised and the lateral and distal convexities of the upper surface were maintained to enable the removal of a single, side-struck flake. The resulting blanks had steep pointed butt shapes and centripetal flake scar patterns on the dorsal face (Sharon and Beaumont, 2006). *Entame* (i.e., cobble opening) flakes have been noted in South Africa (~530 – <408 ka, Caruana and Herries, 2020, 2021; Herries et al., 2022; Caruana et al., 2023), North Africa (1.3 Ma, Gallotti et al., 2021, 2023), and Iberian Peninsula Acheulian sites (Sharon, 2011). *Entame* flakes were obtained by striking a cobble at an obtuse angle to produce a large flake blank with a cortical dorsal face which required minimal modification to be shaped into an LCT (Sharon, 2011). Sharon's (2011) experimental work found that the *entame* method required a degree of planning depth by the knapper to control for the size and shape of raw material packages and determine the location and angle of the percussion blow to detach the large flake. The slab slice method utilises large, flat slabs or cobbles, which were sliced through their thickness to obtain a large flake of a desired morphology (Sharon, 2009). Sharon (2007, 2009; Paddayya, 1977, 1982) found that slice slab LCTs from the Hungsi V site exhibited thick profile morphologies with steep lateral edges, and cortex coverage on the bases. Many of these have two ventral faces and thus resemble a kombewa or "janus" flake (Newcomer and Hivernel-Guerre, 1974, Sharon, 2009).

The advantages of obtaining large flake blanks have been preliminarily discussed. For example, Jones's (1994) replicative experiments highlighted that LCTs made on large flake blanks required less manufacturing time and have a greater ratio of edge length to mass when compared to cobble-reduced pieces. He further observed that shaping cobble blanks required more attention to technically demanding reduction phases, such as thinning, and restricted the overall LCT form. McBrearty (2001) asserted that morphological standardisation and thinness in Middle Pleistocene handaxe assemblages resulted from the use of large flake blanks rather than reduction intensity and/or retouch. Archaeological and experimental studies have stressed the difficulties of handaxe thinning, which is essential to reducing weight and controlling center of mass placement (Callahan, 1979; Shelley, 1990; Winton, 2005; Gowlett, 2006; Stout et al., 2014; Caruana, 2022). Shelley (1990) and Winton (2005) noted that inexperienced knappers tend to have trouble reducing the thickness in bifacial tools, which is often complicated by

the development of pervasive step and hinge fractures. However, [Winton \(2005\)](#) also found that much of the difficulty in thinning was bypassed when novice knappers used flake blanks instead of cobbles or nodules, due to their pre-existing thin forms. In fact, the ability to select an appropriate blank, according to size and shape, for a desired tool form, is considered a measure of knapping expertise ([Callahan, 1979](#); [Madsen and Goren-Inbar, 2004](#); [Sharon, 2007](#)).

Thus, the use of large flake blanks can have a significant impact on LCT reduction processes, specifically for shortcutting the technical demands of thinning procedures and avoiding knapping mishaps. Such advantages are particularly relevant for handaxe production at Amanzi Springs, where previous studies have found that many handaxes were likely discarded before or during thinning. The specific quartzite materials (accounting for > 90 % of all lithologies used at the site) are prone to step and hinge fracturing ([Caruana and Herries, 2021](#); [Caruana, 2022](#); [Herries et al., 2022](#); [Caruana et al., 2022, 2023](#)). Coupled with the technical demands of platform preparation and controlling percussive force during thinning, reducing cobbles was likely significantly challenging at Amanzi Springs. The observed increase in large flake blank use throughout the Area 2 assemblages may therefore relate to 'pre-determining' thinness in LCT morphologies in an effort to avoid pervasive surface flaws (i.e., step and hinge fractures) as distinguished from internal flaws within the raw material ([Caruana et al., 2022, 2023](#)). Below, we test this hypothesis through various qualitative and quantitative analyses to assess the potential effects of large flake blanks use versus cobble reduction on handaxe forms. We also compare different large flake blank types to explore the advantages of investing time and effort in preparing giant cores as a means of attaining desired blank morphologies.

2. Materials

2.1. Amanzi Springs Area 2

The Amanzi Spring site lies ~ 40 km north of Gqeberha (formerly Port Elizabeth) in the Eastern Cape Province of South Africa and consists of twelve inactive spring eyes located on the northern flank of Amanzi hill ~ 2 km south of the Coega River valley ([Fig. 1A](#)) (see [Herries et al., 2022](#); [Caruana et al., 2023](#)). Peninsula Formation Quartzitic Sandstones, derived from the Table Mountain Group (TMG), comprise the dominant raw material type, which were incorporated into the Enon Formation during the pre-Cretaceous period, which is characterised as a thick bedded, poorly sorted conglomerate ([Muir et al., 2017](#); [Herries et al., 2022](#); [Caruana et al., 2023](#)). Acheulian artefacts at Amanzi Springs were manufactured predominantly on Enon quartzite, though silcrete artefacts were also recovered, which derive from a silcrete cap on top of Amanzi hill ([Deacon, 1970](#)). While no large flat natural slabs have been found in the Amanzi Springs assemblages, an abundance of natural quartzite clasts ranging in size from pebbles to boulders are found throughout the landscape surrounding the site ([Caruana et al., 2023](#)). This includes locally available boulder-sized clasts (>25 cm in maximum dimension) that range from tabular to ellipsoidal in both plan and profile, with natural flat surfaces and rounded edges ideal for large flake production ([Caruana et al., 2023](#)).

After preliminary excavations by [Inskeep \(1965\)](#), [Deacon \(1966, 1970\)](#) undertook extensive excavations of two Acheulian-bearing spring eyes (referred to as Area 1 and 2) between 1964 and 1966 for his master's research. [Deacon \(1970\)](#) documented multiple stratified, archaeological deposits including those that contained extensive organic remains, including preserved wood. Within Area 2, three distinct artefactual surfaces (Surfaces 1, 2, and 3) were identified in the 'Deep Sounding' excavation in the central portion of the spring, along with large accumulations of Acheulian material from the northern margins of the spring in the Cutting 5 excavation ([Fig. 1B](#)) ([Deacon, 1970](#)). These deposits were recently dated using a combination of single-grain quartz thermally transferred optically stimulated luminescence (TT-OSL) and

multi-grain K-feldspar post-infrared stimulated luminescence (pIR-IRSL) ([Fig. 1C](#)) ([Caruana et al., 2023](#)). In all cases, the replicate TT-OSL and pIR-IRSL ages for individual luminescence dating samples overlap within their 1 σ errors, and therefore the final sample ages have been calculated using the weighted means of the two sets of ages. The Deep Sounding excavations consist of two sealed surfaces (2 & 3) within a White Sand unit dated to between ~ 534 and 481 ka, within MIS 13 ([Caruana et al., 2023](#)). Surface 1 occurs around 30 cm above luminescence dating sample ASP18-3, which returned an age of ~ 481 ka ([Caruana et al., 2023](#)). While it is thought that the Surface 1 artefacts primarily come from deflation of material that was once in the upper layers of the White Sands before it was truncated, we cannot conclusively rule out material being incorporated onto the surface from units overlying Surface 1 ([Caruana et al., 2023](#)). The marginal Cutting 5 deposits overlie the central White Sand units encompassing material from the bottom of the 'Grey-Black Silts' unit, downward through the 'Brown Humic Sands' to the top of the 'Basal Clay' unit, which has been dated to ~ 408 ka (MIS 11) ([Deacon, 1970](#); [Caruana et al., 2023](#)). In some cases, the artefacts from Cutting 5 appear to represent deflation onto surfaces within the sequence, like the Surface 1 assemblage, but in other cases the archaeology is sealed within the sedimentary units ([Caruana et al., 2022, 2023](#)). However, [Deacon \(1970\)](#) amalgamated artefacts from the different units into one Cutting 5 assemblage, due to the complexity of the stratigraphic sequence ([Caruana et al., 2023](#)). For this study, Surfaces 2 and 3 have been combined due their chronological overlap and similarities in technological features (i.e., Deep Sounding) ([Caruana et al., 2022, 2023](#)).

2.2. The Area 2 assemblage

In total, 89 handaxes, excavated by [Deacon \(1970\)](#) from Area 2, were used in this study, which included 29 specimens from Surfaces 2 and 3 (Deep Sounding), 32 from Surface 1 (including Cuttings 6, 7, 8 and 9), and 28 from Cutting 5 assemblages ([Table S2](#)). The sample of [Deacon's \(1970\)](#) material selected for this study includes only complete handaxes where the blank type and/or giant core reduction method could be determined. This excluded handaxes that were reduced to the point where blank type could not be determined, or handaxes which were broken. Cleavers were excluded due to small sample sizes across all assemblages. All handaxes were made on Table Mountain Group (TMG) quartzite of varying structural qualities ([Herries et al., 2022](#); [Caruana et al., 2023](#)).

3. Methods

The blank types of handaxes were identified using definitions provided by [Isaac and Keller \(1968\)](#), [Paddayya \(1977, 1982\)](#), [McNabb et al. \(2004\)](#), [Sharon \(2007, 2009, 2011\)](#), [Goren-Inbar et al. \(2018\)](#) and [Garcia-Medrano et al. \(2020\)](#), which included cobble and large flake categories. The presence of a ventral surface, or a complete or partial bulb of percussion distinguished large flake blanks, while handaxes with cortex present on both faces indicated a cobble blank. Handaxes made on large flake blanks were further separated by giant core reduction methods, which included slab slice, *entame*, and side, end, and corner stuck blank types ([Figs. S3 – S6](#)). Due to the low number ($n = 3$) of giant cores found in Area 2 ([Fig S1 & S2](#)), we relied on observable diagnostic features that distinguished different types of large flake blanks. Slab slice handaxes were identified by their thick profile morphologies, which had steep lateral edges, and cortical rounded or flat bases ([Sharon, 2007, 2009](#)). Many of these artefacts resemble kombewa or "janus" flakes ([Newcomer and Hivernel-Guerre, 1974](#)), having two ventral faces ([Sharon, 2009](#)). [Sharon \(2007, 2009\)](#) further notes some LCTs were produced with at least one backed edge, giving them a knife-like appearance, which was suggested to relate to the stage within the giant core knapping sequence at which they were detached. The *entame* handaxes were identified by their cortical striking platforms and

minimally reduced dorsal surfaces (Sharon, 2011). We also included an 'indeterminate' large flake category where striking platforms and ventral surfaces could be identified, but not distinguished in terms of giant core reduction method. We identified these handaxes based on the angle of the detachment strike relative to the long axis to the handaxe, which included side, end, and corner struck blanks, following Isaac and Keller's (1968) definitions. We aggregated these indeterminate large flake blank types due to their small sample sizes and the range of potential unifacial and bifacial core design methods from which they may have been produced (Madsen and Goren-Inbar, 2004; Sharon, 2007, 2009).

Diacritical descriptions of handaxe flaking methods are employed, which focus on flaking patterns, volume management and cortex removal are provided for context (de la Torre and Mora, 2018; Santonja et al., 2018; Caruana et al., 2022). Standard metric measurements (mm) were collected using digital calipers, including maximal length, width and thickness, width and thickness for tip, midsection, and basal portions, defined as 1/5, 1/2 and 4/5 of the tool length (Crompton and Gowlett, 1993; Garcia-Medrano et al., 2020). Two-dimensional shape variability was investigated using elongation (L/W) and refinement (W/TH) ratios (Roe, 1968), and the scar density index (SDI) was calculated using flake scar count divided by surface area as a proxy for reduction intensity (Clarkson, 2013; Shipton and Clarkson, 2015). Step and hinge fractures, referred to here as surface flaws (Caruana and Herries, 2021; Caruana et al., 2022), were counted and their average length was calculated for comparison.

Investigation of the morphological variability of the different blank types was conducted using a three-dimensional, semi-landmark-based geometric morphometric shape analysis. Handaxes were scanned using an Artec Space Spider scanner and processed using the Artec Studio 15 Professional software, which produced water-tight, three-dimensional meshes. These meshes were then imported into MeshLab (v.2020.07), where normals were re-calculated and they were orientated before being exported as WRL (Virtual Reality Modeling Language) files. In addition, surface area (cm²) and volume (cm³) measurements were calculated, along with cortex surface area (cm²) on meshes using the Geomagic Warp (v.2017) software. Cortex ratios were calculated as a percentage of total surface area (cortex surface area / total surface area * 100).

AGMT3D software (v.3.1) was used to perform three-dimensional geometric morphometrics shape analysis (3DGM) following established protocols (Herzlinger et al., 2017a; Herzlinger and Grosman, 2018; Herzlinger and Goren-Inbar, 2019, 2020). The AGMT3D software automatically orientates and aligns meshes along their long axis, with handaxe tips orientated upwards. However, for consistency each mesh was rotated depending on the blank type, corresponding to which face of the artefact was analysed first. Large flakes were always orientated with the ventral surface as face A and dorsal face B, whereas, for cobble blanks, the least shaped face of the artifact was designated as face A. After positioning, the landmarks were established within a grid of 50 x 50, resulting in 5000 semi-landmarks per artefact (2500 per face). The semi-landmark coordinates were subject to a generalized Procrustes analysis (GPA) and a principal component analysis (PCA) using the AGMT3D software. These data were also used to determine the degree of bilateral and bifacial symmetry (Herzlinger and Grosman, 2018). A perfectly bilateral or bifacial artefact would reflect a value of 0 in this index, with increasing numbers reflecting less symmetrical shapes. The non-parametric Wilcoxon Rank Sum Test was used to evaluate the statistical significance of mean shape differences between the inter point distances of semi-landmarks samples (Herzlinger and Grosman, 2018; Herzlinger and Goren-Inbar, 2019). The mean handaxe shape per assemblage and blank production method were visualised as two-dimensional hat maps, highlighting the relative variability of landmarks between assemblage groups (Fig S7 – S9). All descriptive statistics analyses were conducted using AGMT3D and R statistics software (R Core Team, 2013).

4. Results

4.1. Linear measurements and diacritical descriptions

Of the 89 handaxes analysed for this study, 76.4 % (n = 68) were made on large flake blanks and the remaining 23.6 % (n = 21) on cobble blanks (Table S2). Within the large flake blank sample, 17.98 % (n = 16) are *entame* flakes, 22.47 % (n = 20) are slab sliced flakes, 15.73 % (n = 14) are side stuck, 3.37 % (n = 3) are end struck and 16.85 % (n = 15) are corner stuck flakes (Table S2). There is minimal variation in handaxe metric variables between assemblages, as well as between the four different blank production methods, with no statistically significant differences identified (Figs. 2 & 3; Table S1). Scar density index (SDI) values also show homogeneity across all three assemblages, with median values in the range of 0.66 to 0.81 (Table S1). Similar SDI median values are seen for each of the giant core reduction methods, ranging from 0.68 to 0.82 (Table S1). Cutting 5 handaxes show higher median elongation and refinement values, as well as the lowest median cortex percentage, but display the most intra-assemblage variability (Fig. 2D & E). Slab Slice blanks present the lowest cortex percentage median value and least variability in cortex coverage of all core reduction methods (Fig. 3J). The Deep Sounding (Surfaces 2 and 3) present the lowest median tip widths, but the highest median tip thickness value, suggesting more pointed tips forms (Table S1). In addition, cobble blanks have the highest mean values for average flaw length, and the longest maximum step scar length (Table S1).

4.2. Diacritical handaxe descriptions

4.2.1. Bifacial cobble reduction

Twenty-one handaxes were made directly on cobble blanks, averaging 134.19 mm in length, 84.16 mm in width and 53.36 mm in thickness, with the smallest mean mass at 617.61 g. Cobble blank selection prioritised naturally elongated tabular to ellipsoidal shapes in both plan and profile, with rounded edges (Caruana et al., 2023). Experiments have shown that cobble blanks tend to exhibit thick rounded or square edges, which can make the beginning of bifacial reduction sequences difficult (Callahan, 1979; Jones, 1994). Handaxe manufacture on cobbles in the Area 2 sample was focused primarily on one or two series of bifacial flake removals around the margins of the blank, perpendicular to the long axis, with a noticeable lack of extensive thinning to manage volume. Similar patterns are noted in the Area 1 handaxe assemblage (Herries et al., 2022). Flaking was concentrated in the top half of the tool, with minimal to no flaking in the basal portions (Fig. 4C, Fig S3). All cobble-reduced handaxes have convergent tip shapes, and seventeen with convex butt shapes that preserve the morphology of the original cobble blank. Cobble blanks were first shaped during a roughing out stage, with knapping sequences initiated on the flatter surface to establish platforms and aid volume removal from opposing faces (Newcomer, 1971; Whittaker, 1994). Following this, a short sequence of flake removals on the opposing faces established a bifacial edge, which was followed by a series of larger invasive flake scars to start removing cortex and volume around the tip. A secondary shaping sequence or small retouch scars were used to regularise areas along the edges and tip (Fig. 4C).

4.2.2. *Entame* blanks

Sixteen handaxes were produced on *entame* flakes, averaging 153.39 mm in length, 94.43 mm in width, 50.59 mm in thickness, with the highest mean mass of all blank production methods at 805 g. The handaxes made on *entame* flakes show the most variability in length, ranging from 97.21 to 208.48 mm (Table S1). Sharon (2011) suggested that the *entame* flaking method is only productive with flatter cobbles and boulders, which allow for flakes to be stuck at obtuse angles deeper into the body of the raw material package. If the cobble or boulder is too spherical, the *entame* flake blanks produced are too thick to be shaped

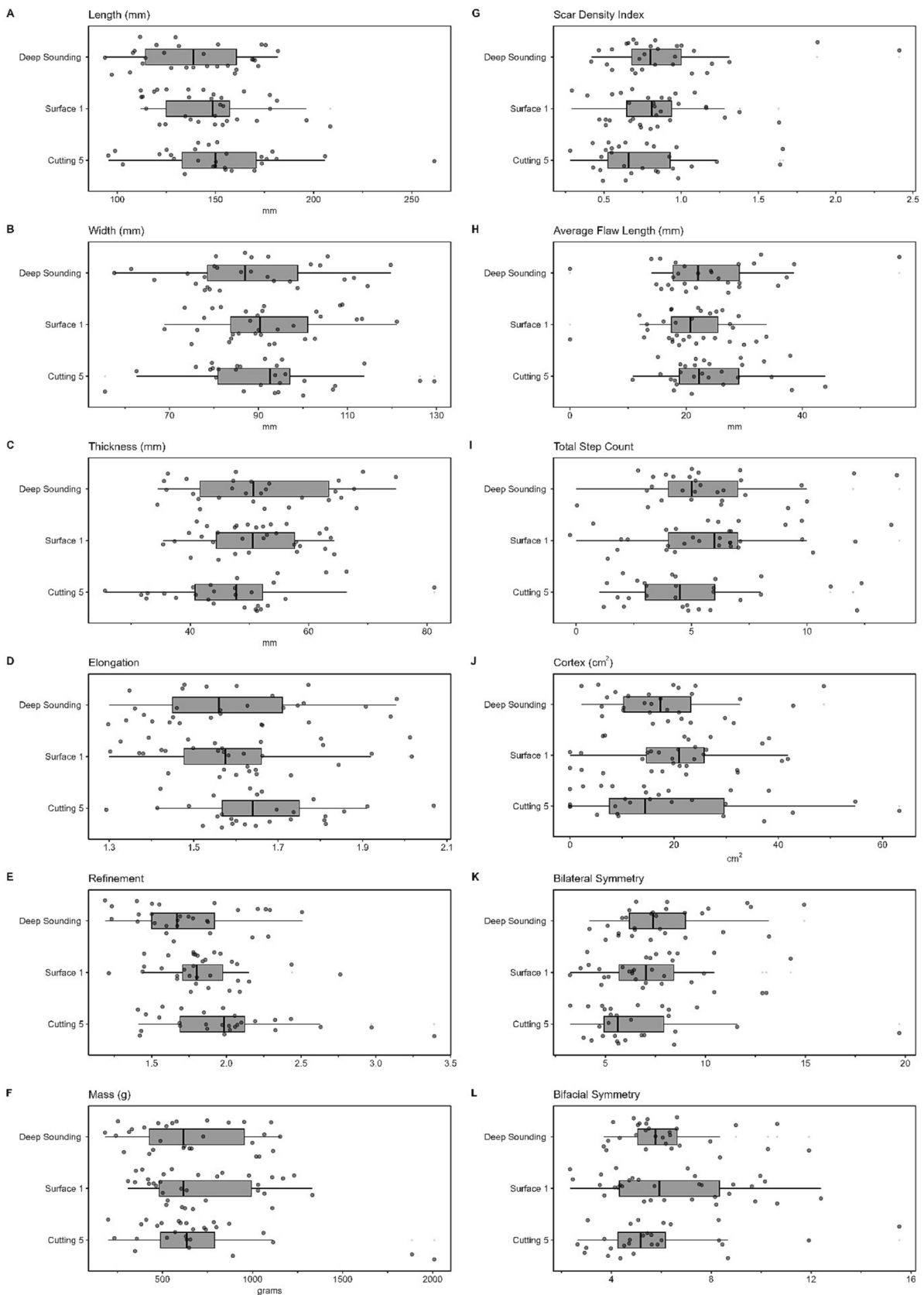


Fig. 2. Boxplots graphs displaying recorded attributes for handaxes from Cutting 5, Surface 1 and the Deep Sounding (Surface 2 & 3) from Area 2.

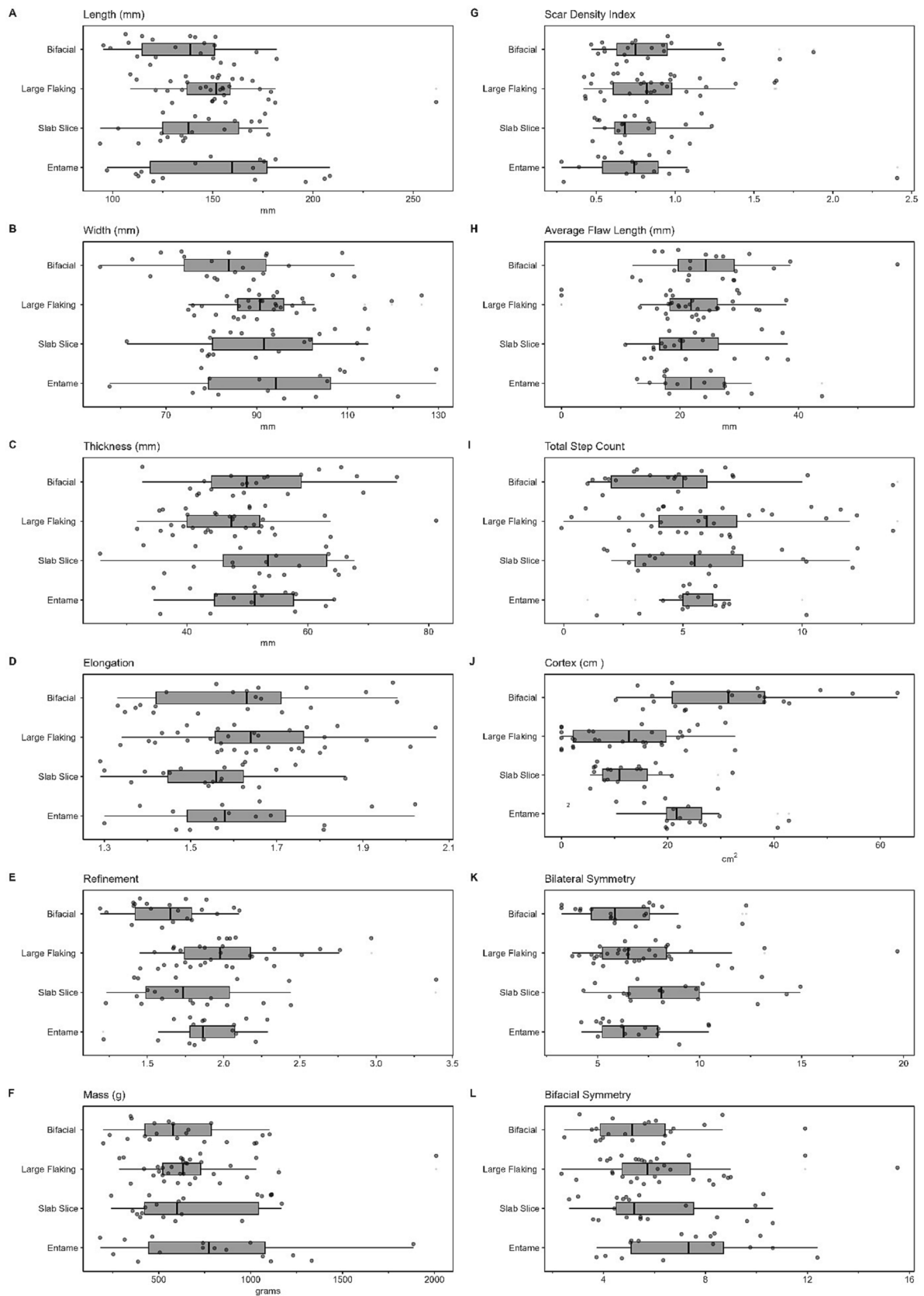


Fig. 3. Boxplots graphs displaying recorded attributes for handaxes blank types from Area 2.

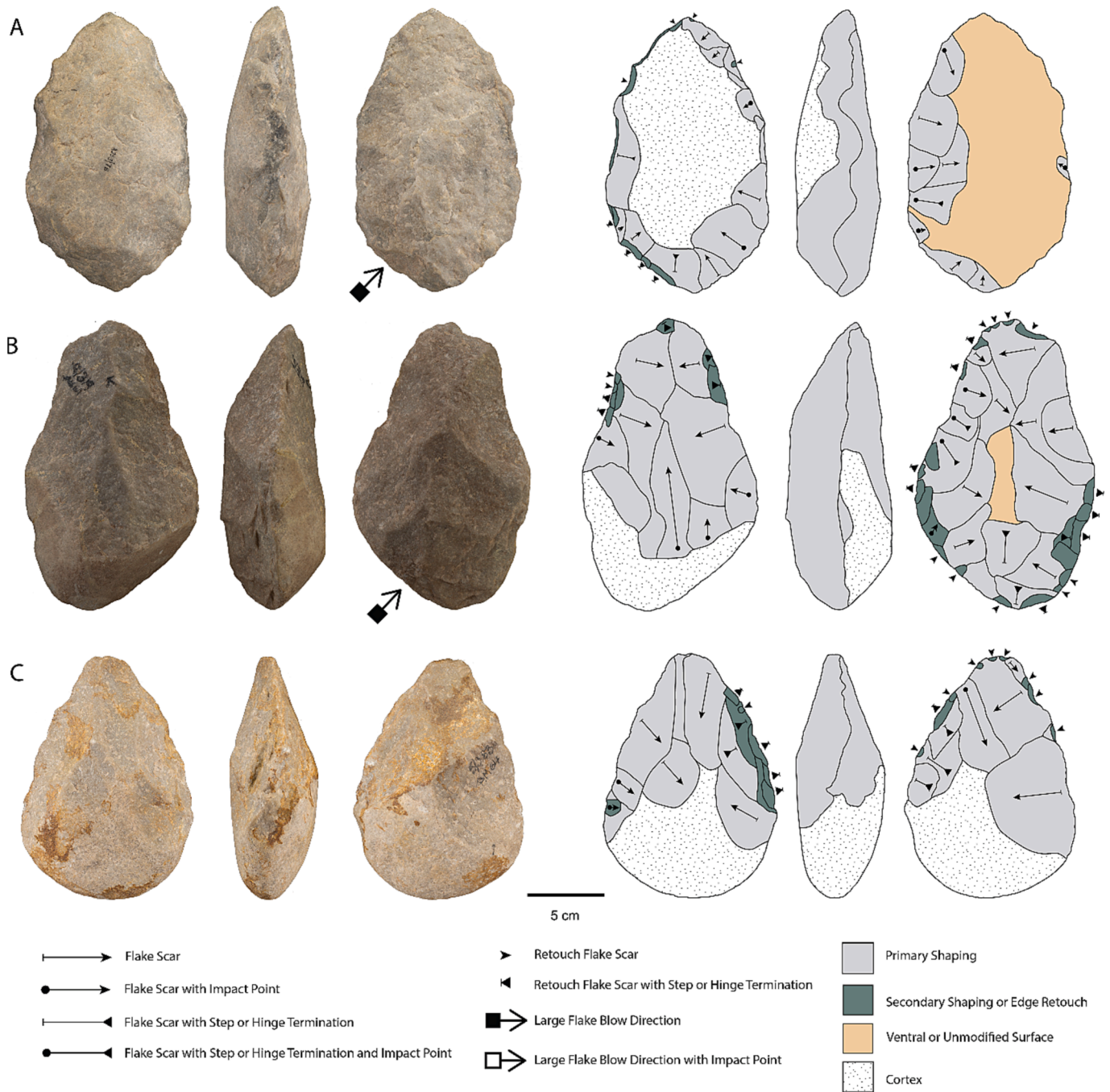


Fig. 4. Area 2 handaxes on large flakes and cobble blanks (A) *Entame* flake, (B) Slab Slice flake, (C) Bifacial cobble reduction.

into LCTs (Sharon, 2011). Although the degree and intensity of flaking vary across the sample, the majority of *entame* handaxes exhibit generalised convergent tips, with straight outline profiles. Seven of these handaxes preserve a cortical platform, with the remaining nine having been removed by a short series of unifacial flakes around the margins. Fourteen handaxes show dorsal flake removals, which are primarily concentrated in the top half of the tool, to remove cortex and establish a bifacial edge (Fig. S4B). Two handaxes have a short, overlapping unifacial flaking sequence around the circumference of the dorsal face (Fig. 4A, Fig. S4C). Of the sixteen *entame* handaxes, eleven have residual cortex in their bottom halves, mainly located in central and basal portions, while the remaining five have cortex that covers most of the dorsal surface. Flaking on the ventral surface is associated with bulb trimming or lowering the bifacial edge deeper into the dorsal volume. Seven

handaxes show intensive flaking on the ventral surface, with either a sequence of regularly spaced, marginal invasive flakes around the circumference or one-to-two large flakes that penetrate the midline of the tool. One artefact is unifacially flaked, with two series of flake removals concentrated around the tip and medial edges (Fig. S4A). The remaining eight have minimal flaking on the ventral surface.

4.2.3. Slab slice blanks

Twenty handaxes were produced on slab sliced flake blanks, of which three different handaxe morphologies were identified based on the point in the knapping sequence at which they were discarded (Sharon, 2009; Goren-Inbar et al., 2011). No giant cores exhibiting slab sliced morphology have been recovered from Area 2 excavations to date, and as such, identification of this core reduction method is based on the

characteristics of the handaxe blanks themselves (Sharon, 2009; Goren-Inbar et al., 2011). Sharon (2007, 2009) noted that slice slab LCTs from the Hungsi V site exhibit thick profile morphologies, with steep lateral edges, and cortical rounded or flat bases. Many of these artefacts resemble kombewa or “janus” flakes (Newcomer and Hivernel-Guerre, 1974), having two ventral faces (Sharon, 2009). Additionally, Sharon (2007, 2009) notes some LCTs were produced with at least one backed edge, giving them a knife-like appearance, which was suggested to relate to the stage within the giant core knapping sequence at which they were detached.

Three handaxes from Area 2 have a shoulder or initial slice flake morphology (Paddayya et al., 2006; Sharon, 2009; Goren-Inbar et al., 2018) and preserve the corner of the original raw material nodule or slab

(Fig. S5B). These handaxes show that the large flake blow was struck perpendicular to the long axis of the tool using a naturally flat portion of the original nodule or slab as a platform. Cortex is predominantly preserved in the base of these tools around the bulb, and along one margin on the dorsal face. Flaking patterns are primarily restricted to the top half of the tool (i.e., tip shaping) to establish a bifacial edge on one or both margins. Nine handaxes are characterised by either one large removal on the dorsal surface, or two large removals resembling a “wedge” morphology (Goren-Inbar et al., 2018), with subsequent primary flaking and secondary shaping patterns not penetrating past the midline of the tool (Fig. S5A). Volume is distributed through the length of the tools, and cortex is preserved where the blank was struck, with a bifacial edge running the circumference of the tool stopping at the

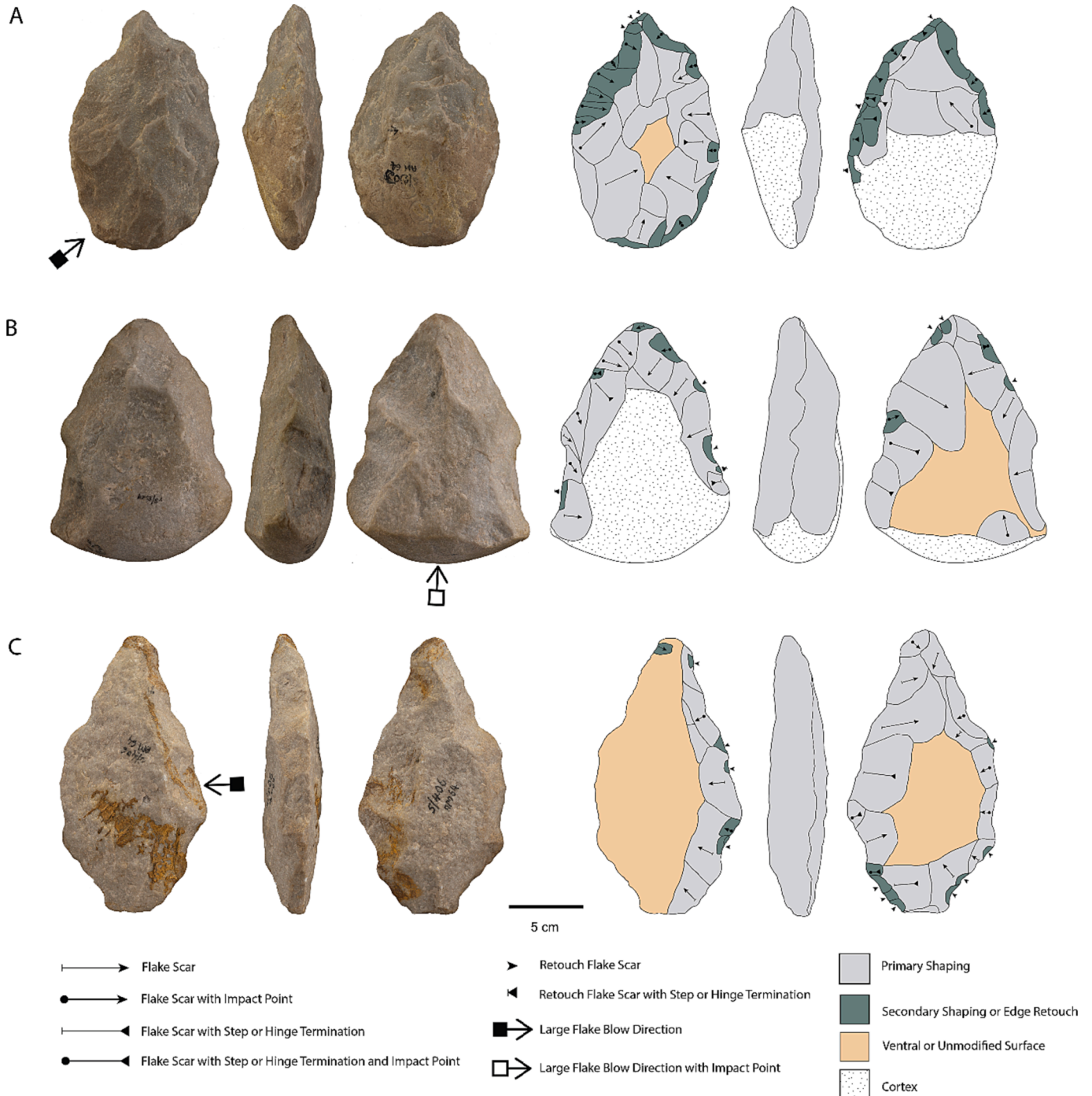


Fig. 5. Area 2 handaxes on large flake blanks (A) corner struck flake, (B) end struck flake, (C) side struck flake.

cortical base. The remaining six handaxes are characterised by their convergent plan shapes with tapered profiles around the tip with volume primarily situated in the basal portions (Fig. 4B, Fig. S5C). Flaking patterns rarely penetrate past the midline of the tool, with a secondary shaping sequence or small edge retouch scars used to regularise areas along the edges and tip.

4.2.4. Large flake blanks

Thirty-two handaxes were produced on either end, side, or corner struck blanks (Fig. S6). Three handaxes were made on end struck flakes, two of which preserve cortical platforms. Flaking patterns are restricted to the margins, with flake removals located on both faces to establish a bifacial edge and tip. All three handaxes have convergent tips and convex butt shapes, preserving cortex in the lower half of the dorsal face of the flake blank. Flake scars do not penetrate to the midline on two handaxes, except for the upper 5th of the tool to define a tip (Fig. 5B, Fig. S6A). Small secondary shaping scars were used to trim the bifacial edges, although no attempts were made to thin volume on the dorsal face of the flake blank. One handaxe has two opposing large preferential flake scars on the ventral face which penetrate past the midline, perpendicular to the long axis of the tool (Fig. S6B).

Fourteen handaxes were produced on side struck flakes, with thirteen showing trimming of the bulb of percussion and platform on the ventral surface. Twelve of these handaxes had cortex remaining, primarily located around the point of percussion or on the lower half of the dorsal face of the flake blank. Flaking patterns are mostly concentrated

around the lateral margins, with short removals that do not penetrate past the midline or either the ventral or dorsal face (Fig. S6F). Nine handaxes have one or two flake scars that penetrate the midline on the dorsal face, although most of these are from previous removals during the initial giant core reduction sequence to obtain blanks. Five handaxes exhibit a unifacially shaping strategy, using the flat ventral surface of the flake blank as a platform to strike of a series of continuous short marginal flakes along the length of edge into the dorsal face. These handaxes were rotated, repeating the same flaking strategy, although using the dorsal face as the platform to strike of a series of continuous short marginal flakes into the ventral face (Fig. 5C, Fig. S6E).

Fifteen handaxes were produced on corner struck flakes, with nine showing bulb and platform trimming. Thirteen of these handaxes preserve cortex, primarily located around the point of percussion or on the lower half of the dorsal face. All handaxes exhibit convergent tip shapes, with a range of butt shapes. Seven have one or two large, wide flake scars on the dorsal surface of the flake blank that penetrate to the midline in the top half of the tool, followed by marginal flaking patterns along one or both edges (Fig. S6D). Flaking on the ventral surface is either restricted to platform trimming to even out volume across the blank, or a short invasive flaking sequence along one or both margins to establish a bifacial edge. Small, secondary shaping scars were used to trim the bifacial edges, with no attempts were made to thin the dorsal face. Two handaxes exhibit the continuous unifacial edge shaping strategy, whereby the dorsal or ventral face was used as a platform to strike of a series of short marginal flakes into the opposing face. The final

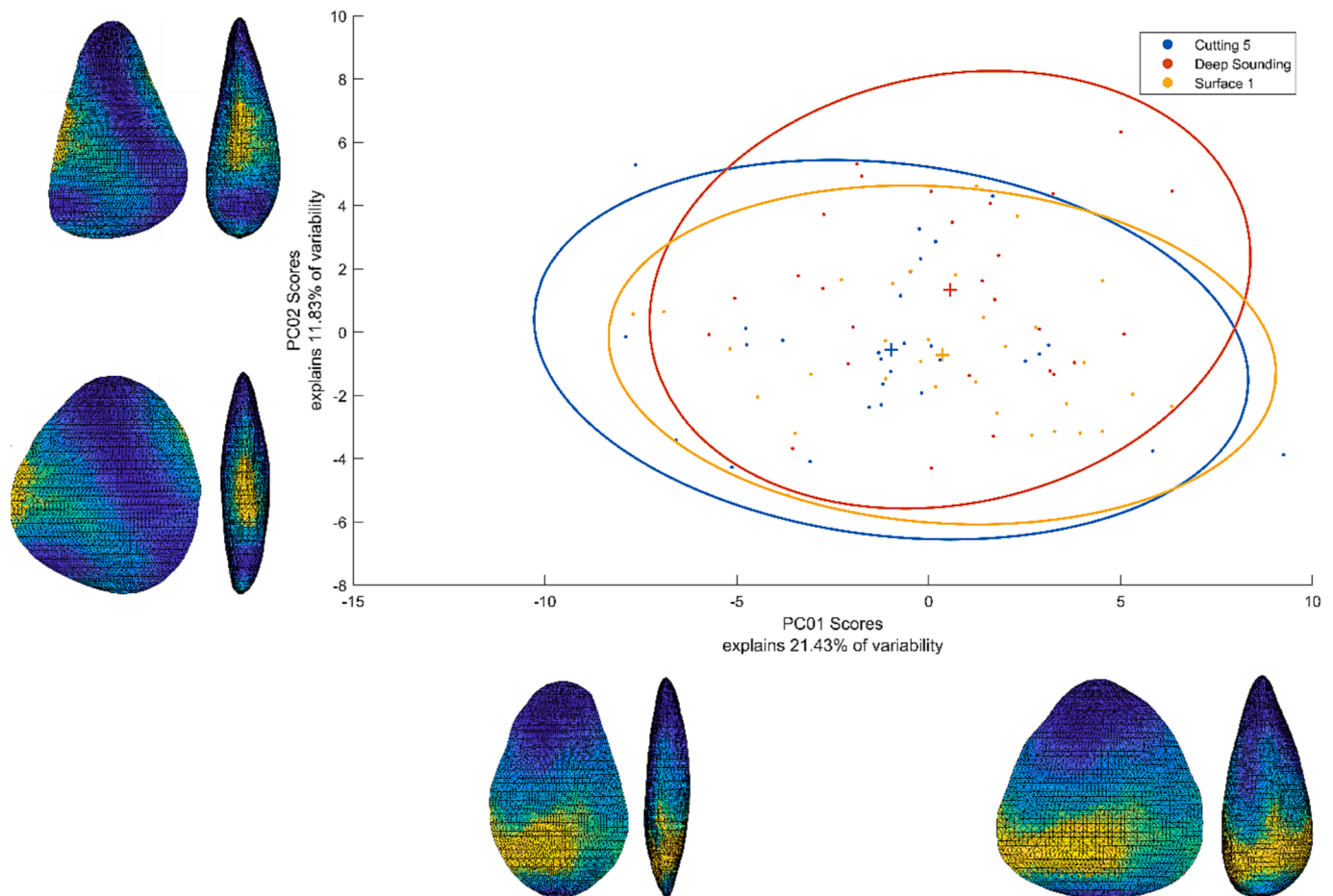


Fig. 6. Scatterplot of first two principal components of the Area 2 Cutting 5, Surface 1 and Deep Sounding (Surface 2 and 3) handaxe assemblages. Ellipses represent 95% confidence ellipses. The illustrations on each PC axis represent the shape trend of the principal component.

six handaxes show intensive flaking on both faces, with a more symmetrical volume distribution throughout the blank. A primary, followed by a secondary shaping series is exhibited across both faces with small edge retouch scars were used to form the edges and tip (Fig. 5A, Fig. S6C).

4.3. Three-Dimensional morphological analysis

Principal component analysis on the 89 scan meshes produced 88 principal components (PCs) with 90.11 % of variation explained by the first 25 PCs. Together PC1 (21.43 %) and PC2 (11.83 %) explained the first 33.27 % of the total morphological variability (Figs. 6 & 7). There is significant morphological overlap between all three samples, with the Surfaces 2 and 3 (Deep Sounding) handaxes loading stronger positive influence on PC2 (Fig. 6). Cutting 5 and Surface 1 occupy a similar space, with Cutting 5 loading slightly stronger negative influence on PC1. PC1 represents a shape trend ranging from thicker to thinner blank morphologies and a decrease in the width in the bottom third of the artefact. PC2 represents pointed to ovate tip shapes, with thinner distal morphologies loading on the negative axis. Fig. 7 displays PCA results comparing different large flake and cobble-reduced handaxes. Again, all four samples occupy a similar morphological space, although bifacial cobbles and slab slice flakes are slightly more skewed towards the positive end of PC1 and PC2, showing higher proportions of pointed tip morphologies with mass distributed more towards the basal end of the artefact. Cobble-reduced handaxes load on the positive ends of PC1 and

PC2, reflecting a higher prevalence for shaping around the tip portions of the tool, with basal regions largely left unshaped. Similarly, most of the mass and cortex in slab slice handaxes is centred in the basal portions, resembling classic cheese wedge shapes (Sharon, 2007, 2009). End, side, and corner-struck flake blanks load towards the negative end of PC1, with more elongated and thinner morphologies. *Entame* flake blanks show an evenly distributed spread of morphological variability across PC1 and PC2, indicating a more standardised final shape.

Assemblage level differences in mean shape variation between flake and cobble blanks were tested using the parametric Wilcoxon rank-sum test, which returned a significant result (rank sum = 6747, $n_1 = 21$, $n_2 = 68$, $p < 0.01$) (Table S3). The mean shape differences show that cobble blanks are more variable in the mid-section portions, whereas large flake blanks show the most variation in both the left and right portions of the basal region (Fig. S7). Cutting 5 handaxes show the lowest shape variability value (7.05), with thinner and elongated shape types, compared to the Surfaces 2 and 3 handaxes, which show a larger proportion of pointed short shapes, with maximum thickness located in the bottom half of the tools (Table 1). A statistically significant difference was observed between the mean shape of the Surfaces 2 and 3 and Cutting 5 samples (rank sum = 2914, $n_1 = 28$, $n_2 = 29$, $p = 0.03$), whereas the mean shape between the Surfaces 2 and 3 and Surface 1, and Surface 1 and Cutting 5 show no significant differences (Table S3). Further examination of the spatial distribution of the overall mean shape shows that Cutting 5 handaxes differ both in the thinness of the blank, and along the lateral edges in the bottom third of the tools (Fig. S8),

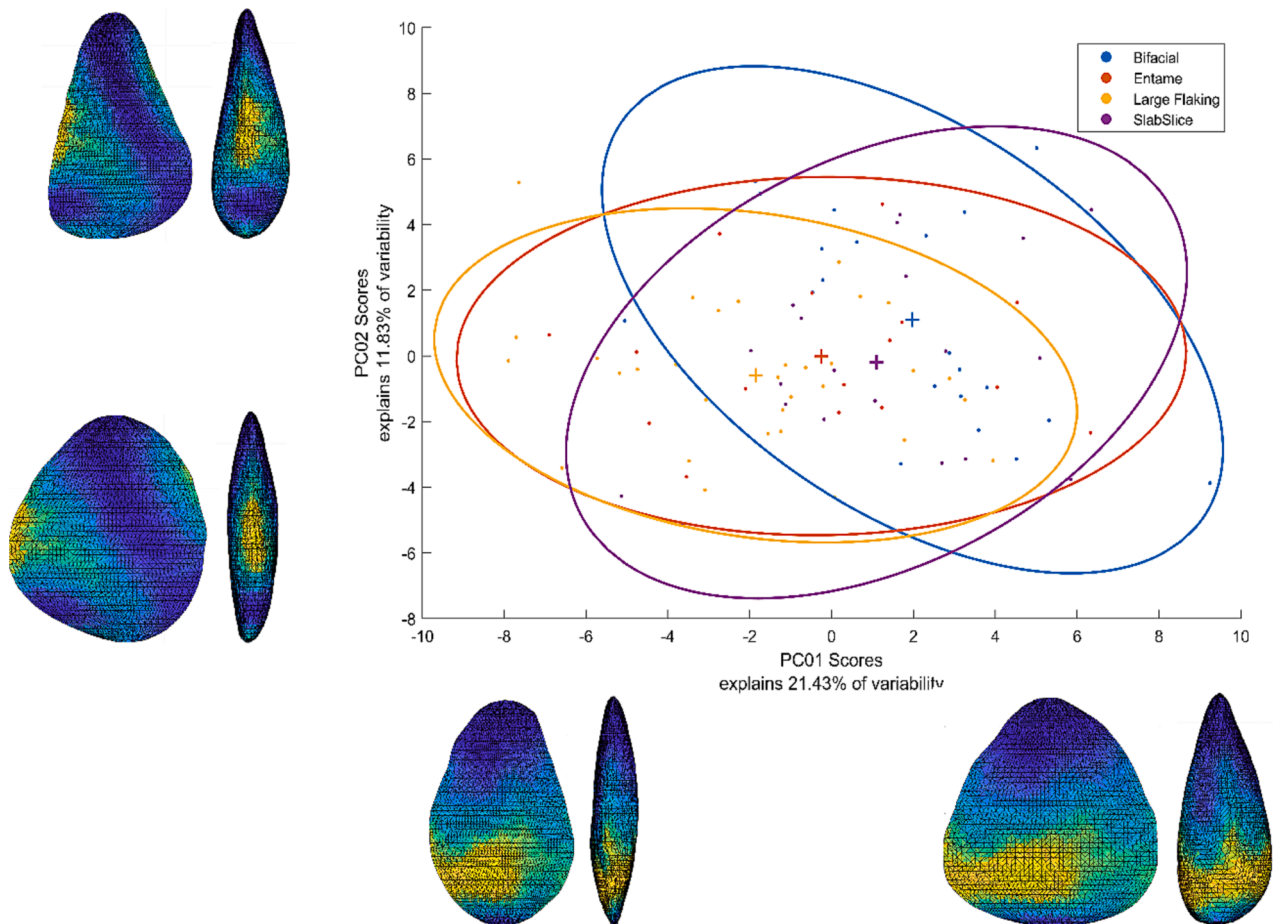


Fig. 7. Scatterplot of first two principal components by handaxe blank type. Ellipses represent 95% confidence ellipses. The illustrations on each PC axis represent the shape trend of the principal component.

Table 1

Shape variability and distribution of morphological variability across three spatial dimensions in Area 2 handaxes.

	Cutting 5	Surface 1	Deep Sounding	Cobble Bifacial	Entame	Large Flaking	Slab Slice
N	28	32	29	21	16	32	20
Shape Variability	7.05	7.21	7.76	7.30	7.04	7.00	7.47
% Caused by X (width)	43.67	38.77	39.36	43.91	41.09	46.09	37.66
% Caused by Y (Length)	3.89	3.50	1.96	2.78	3.43	3.22	3.02
% Caused by Z (Thickness)	52.44	57.73	58.67	53.31	55.48	50.70	59.32

compared to both the Surfaces 2 and 3 and Surface 1 handaxes, which tend to be thicker in the medial and basal portions of the tools (Fig. S8). All three assemblages exhibit a range of pointed tip morphologies with minimal differences in the top third of the tools, with the Cutting 5 handaxes showing the most tip shape variability (Fig. S8). With regards to both bilateral and bifacial symmetry, the Cutting 5 sample has the lowest mean values between the three assemblages (Table S6 & S7), with a statistically significant deviation from bilateral symmetry (rank sum = 656, $p = 0.01$) (Table S4). However, the degree of deviation from bifacial symmetry between the three assemblages is not significant (Table S4 & S5). This could suggest that symmetry in both plan and profile was not a priority for Amanzi knappers when manufacturing handaxes (Caruana, 2020, 2021).

In terms of reduction methods, the three large flaking methods and cobble bifacial methods show a similar degree of shape variability, although the large flaking method (end, side and corner struck flakes) shows the lowest shape variability value (7.00) (Table 1). Again, however, there was a statistically significant difference in the amount of shape variability between handaxes made by direct bifacial reduction of cobbles and the large flaking and *entame* methods (end, side, and corner struck flakes: rank sum = 2121, $n_1 = 21$, $n_2 = 32$, $p = <0.1$; *entame* flakes: rank sum = 1141, $n_1 = 21$, $n_2 = 16$, $p = <0.1$) (Table S3). Further examination of distribution of overall mean shape variability across these handaxes shows that cobble blanks exhibit the most variation along the mid-section edges (Fig. S9), whereas both large flakes and *entame* blanks are more variable around the proximal areas of the tools. *Entame*, slab slice and large flakes also deviate from cobble blanks, with more centralised variation in the bottom half of handaxes, which relates to the configuration of the volume and the position of the bulb of percussion. Furthermore, a statistically significant difference was observed between the mean shape of large flakes and slab slice blanks (RS = 2378, $n_1 = 32$, $n_2 = 20$, p value = 0.02) (Table S3). Examination of the mean shape shows a more even distribution of mass throughout slab slice blanks compared to large flakes, which preserves more mass in the medial portions (Fig. S3). In addition, the bifacial edges of the large flake blanks appear more sinuous, especially around the medial to basal portions, which could relate to the removal or trimming of the bulb of percussion in both side and corner struck flake.

The overall morphological variation in the Area 2 handaxe assemblages is mostly concentrated in relative width and thickness dimensions (Table 1). However, the distribution of morphological variability between relative length, width and thickness is mostly standardized between assemblages, with few notable exceptions. The Surfaces 2 and 3 (Deep Sounding) presents low values of variable length compared to the other assemblages, which could relate to the higher number of cobble blanks in the assemblage (Table S2). Slab slice blanks show relatively low values of length and width but the highest value for thickness, suggesting that slab slice blanks vary little in overall plan shape (Table 1).

5. Discussion

The production of handaxes on large flakes can be achieved using a range of initial blank morphologies or different giant core methods, enabling flexibility in operational sequences from procurement, initial core reduction, through to the handaxe manufacturing and shaping

processes. This is especially the case for cleaver production, which entails both pre-planning and configuration of knapping surfaces to detach a large flake with predetermined characteristics (Texier and Roche, 1995; Herzlinger et al., 2017b). However, our results suggests that certain blank characteristics and morphologies were specially selected by Amanzi knappers for producing handaxes.

5.1. Benefits of large flake blanks for handaxe production

5.1.1. Initial blank selection

Handaxe morphological variability across all Area 2 handaxe assemblages was influenced by a range of technological procedures, the most prominent of which was the degree of shaping, while handaxe profiles and overall thickness appear to be more influenced by initial blank selection. Thinning a handaxe is considered to be the mostly technically difficult stage of the manufacturing process, involving a series of hierarchical knapping routines to detach invasive flakes which penetrate the midline of the tool to remove mass and manage surface convexities (Newcomer, 1971; Callahan, 1979; Caruana, 2020, 2021, 2022; Stout et al., 2014; Sipton, 2018). To successfully do this, knappers must identify and manage internal flaws and prevent the development of extremely thick edges which can lead to flaking accidents resulting in step and hinge fractures (Callahan, 1979; Shelley, 1990; Jones, 1994).

Thus, initial blank selection and the primary phase of handaxe reduction have a substantial impact on the later stages of the manufacturing process, including the ability to remove mass and thin these tools (Callahan, 1979; Madsen and Goren-Inbar, 2004; Winton, 2005; Sharon, 2007). For example, the roughing out phase leaves the knapper with an intermediate handaxe form, which requires judgement on whether to precede with further shaping and thinning (Winton, 2005). This initial shaping phase is the most morphologically variable stage of handaxe manufacture, and imperfections in raw materials must be removed to proceed with secondary shaping and thinning. The removal of cortical surfaces, especially for cobble blanks, during this early roughing out phases is critical in both forming the handaxe plan shape and establishing the bifacial edges (Newcomer, 1971; Callahan, 1979). The interplay of these issues can be seen in the Area 2 handaxe assemblage, with several handaxes documenting the earlier phases of reduction, and not progressing through to a secondary shaping or thinning phase, due to the development of large surface flaws or being unable to remove cortex or centralised mass on the blank.

5.1.2. Morphological standardisation

Large flakes are the most common blank type used for handaxe manufacture across all three assemblages in Area 2, while the use of cobble blanks decreases in the younger, Cutting 5 (<408 ka) assemblage. The range of technological procedures used to detach large flakes at Area 2 resulted in similar handaxes forms. To some extent, the shape and size of raw material packages must have played a role in determining handaxe morphologies, which is reflected in the homogeneity of metric measurements across the assemblages and different blank types (Figs. 2 & 3). Handaxes manufactured on cobble blanks follow a standardised procedure, whereby the basal portion is largely left unworked, with most of the shaping located on the tip and mid-sections. Alternatively, primary flaking patterns, as well as secondary shaping,

on flake blanks show a tendency towards developing or extending the perimeter of the bifacial edge compared to modifying the volume of the blank or outline symmetry.

The results of the 3DGMM shape analysis show that there is substantial overlap in morphology in the first two principal components, which could be the result from high intra-group morphological variability (Herzlinger and Goren-Inbar, 2020). However, there are clear statistical differences in the mean shape between the ~ 530–481 ka Surface 2/3 (Deep Sounding), which show a tendency for thicker and more pointed handaxe forms, and the < 481–<408 ka Surface 1 and < 408 ka Cutting 5 handaxes, which show less standardisation in tip morphology but thinner longer flake blanks. Mean shape distribution is mostly standardised in plan-view, although a decrease in overall handaxe thickness is visible through time, starting from Surface 2/3 (Deep Sounding), through Surface 1 and into Cutting 5 (Fig S2). In contrast, the significant morphological differences between cobble blanks and the other three large flaking methods were likely related to both the convergent tip morphology, treatment of lateral edges, and the preservation of mass in the bottom half of cobble handaxes.

5.1.3. Surface flaws and bifacial edge development

Previous studies have suggested that the interplay between raw material quality and knapping mistakes during manufacturing processes often led to early discard of handaxes during primary shaping phases at Amanzi Springs (Caruana and Herries, 2020, 2021; Caruana, 2021; Caruana et al., 2022, 2023). Callahan (1979) noted that hard-hammer percussion on quartzites often produced incipient step and hinge fractures due to internal raw material flaws. Likewise, Jones (1994) highlights that the tough, coarse-grained internal structure of quartzite often made the detachment and shaping of large flakes difficult due to crushing and/or splitting of flakes when inadequate percussive force was used. Step fractures also tend to propagate with the retouching of more obtuse edge angles during LCT shaping (Jones, 1994). Caruana et al. (2022) identified a trend in LCT flaking patterns in the younger Surface 1 and Cutting 5 assemblages, where changes in flaking angles and additional shaping phases were used to isolate and remove surface flaws. While surface flaws are documented in all Area 2 handaxe assemblages, cobble blanks show a tendency for slightly larger average flaw lengths. Furthermore, both Callahan (1979) and Jones (1994) state that cobble blanks tend to exhibit thick rounded or square edges, which can make the beginning of bifacial reduction sequences difficult. As such, the toughness of the Enon quartzite may have inhibited both the successfully opening of cobbles and the ability to detach long invasive flakes to penetrate the midline. However, the increase in large flake blank use at Area 2 seems to only mitigate or shorten the knapping sequences related to creating a thin lenticular handaxe while still experiencing surface flaws.

5.1.4. Extent of cortex coverage

While the extent of cortex coverage on the Area 2 handaxe varies, only a few have been completely stripped of cortical surfaces. The presence of residual cortex likely relates to the raw material toughness and/or the size and shape of the original blank, with larger blanks requiring more flake removals to fully remove the cortex. However, the full decortication of cobbles was seldom achieved by the Amanzi knappers when manufacturing handaxes, regardless of blank size. Moreover, large flake blanks tended to retain residual cortex on the dorsal surface, usually at the proximal end, suggesting that relatively short core reduction sequences were used to obtain the large flake blanks prior to handaxe manufacture. The location and amount of cortex, coupled with the specific shaping strategies used for each blank type, suggest that the Amanzi knappers focused their efforts on modifying tips while leaving base ends thick and relatively unmodified. Although the presence of cortex may also relate to a functional aspect of handaxe manufacture (Gowlett, 2006), slab slice blanks appear to have circumvented the need to remove extensive amounts of cortex.

Slab slice blanks showed the lowest cortex range for all blank types, with residual cortex primary located around the basal portions of the tool. Sharon and colleagues (2007, 2009; Goren-Inbar et al., 2011) report that obtaining large flake blanks with slab type morphologies is highly efficient, allowing the knappers to exploit the natural geometry of the raw material clast with minimal preparation. Flake blanks could be struck perpendicular to the thickness of the clast, using the natural flat surface of the slab or cobble as a platform (Sharon, 2009). Sharon (2009) further notes that many giant core methods were adapted to the natural shape of the local raw material, including both slab slice and *entame* methods. While no large flat natural slabs have been found in the Amanzi Springs assemblages, an abundance of natural quartzite clasts ranging in size from pebbles to boulders are found throughout the landscape surrounding the site (Caruana et al., 2023). Locally available boulder-sized clasts (>25 cm in maximum dimension) range from tabular to ellipsoidal in both plan and profile, with natural flat surfaces and rounded edges ideal for large flake production (Caruana et al., 2023). As such, the adaptation of giant core reduction methods to local raw materials was critical for the Amanzi knappers to overcome the challenges related to manufacturing handaxes directly on cobbles (Caruana and Herries, 2021; Caruana et al., 2022). Instead, slab slice and *entame* methods presented the knapper with both thinner blank morphologies and a consistency in cortex coverage that required minimal modification.

6. Conclusion

The results of this study indicate that operational sequences used to manufacture handaxes by Middle Pleistocene (~530 – <408 ka) hominins at Amanzi Spring Area 2 incorporated flexibility in blank production by using a variety of large flake core reduction strategies to exploit the natural geometry of raw material packages. This enabled the production of a variety of large flake blank types that offered knappers the opportunity to shortcut both the thinning and decortication phases of handaxe manufacture. In contrast, handaxe manufacture directly on cobble blanks required the knappers to adapt their flaking strategy to the constraints of available raw material clasts. Although the use of cobbles as blanks typically produced longer surface flaws early in the reduction process, all blank types appear to have produced high rates of surface flaws during handaxe manufacture. An increase in the use of large flake blanks in the younger Surface 1 and Cutting 5 assemblages (481 – <408 ka) resulted in a decrease in overall handaxe thickness. It is therefore possible that knappers, through time, increased large flake blank use to shortcut the challenges associated with extensive thinning (Callahan, 1979; Shelley, 1991; Caruana and Herries, 2021). The increase in the variety of large flake production methods in the Surface 1 and Cutting 5 assemblages allowed the Amanzi knappers to be more selective about raw material shapes and sizes, and secondly, produce blanks with standardized characteristics and morphologies, which could be predictably manufactured into handaxes.

CRediT authorship contribution statement

Coen G. Wilson: Conceptualization, Data curation, Formal analysis, Investigation, Methodology, Software, Visualization, Writing – original draft, Writing – review & editing. **Matthew V. Caruana:** Conceptualization, Funding acquisition, Formal analysis, Investigation, Methodology, Supervision, Writing – original draft, Writing – review & editing. **Alexander F. Blackwood:** Conceptualization, Funding acquisition, Investigation, Supervision, Writing – review & editing. **Lee J. Arnold:** Funding acquisition, Supervision, Writing – review & editing. **Andy I.R. Herries:** Conceptualization, Funding acquisition, Investigation, Supervision, Visualization, Writing – review & editing.

Declaration of competing interest

The authors declare that they have no known competing financial interests or personal relationships that could have appeared to influence the work reported in this paper.

Data availability

Data will be made available on request.

Acknowledgements

Research at Amanzi Springs is funded by Australian Research Council Discovery Projects (DP170101139 and DP200100194) awarded to AIRH and a National Geographic Explorer grant (GR-000046142) to AIRH, MVC, LJA, and AFB. The Artec Space Spider scanner was funded through AIRH's Australian Research Council Future Fellowship grant (FT120100399). CW was supported by an Australian Government Research Training Program Scholarship while completing a PhD through La Trobe University. We would like to thank the landowners, Phillip and Clyde Niven for granting us access to the Amanzi Springs archaeological site. All research was carried out through permit number 2/2/AMP-PERMIT/16/09/110 issued by the Eastern Cape Provincial Heritage Authority (ECPHRA). We would like to thank Sello Mokhanya for his assistance with permitting at ECPHRA. We are also grateful to Celeste Booth from the Albany Museum in Grahamstown for her continued support of our research. We are especially grateful to the Amanzi Town community members, including Mrs. Regina Komazi and Mr. R. Mstwana, for their continued support of our research. We finally express our appreciation to the three anonymous reviewers, whose comments and suggested changes improved the quality of this manuscript.

Appendix A. Supplementary data

Supplementary data to this article can be found online at <https://doi.org/10.1016/j.jasrep.2024.104393>.

References

- Alimen, M.H., 1978. L'évolution de l'Acheuléen au Sahara Nord-Occidental (Saoura, Ougarta, Tabelbala). CNRS, Paris.
- Archer, W., Braun, D.R., 2010. Variability in bifacial technology at Elandsfontein, Western cape, South Africa: a geometric morphometric approach. *J. Archaeol. Sci.* 37, 201–209.
- Barham, L., Duller, G.A.T., Candy, I., Scott, C., Cartwright, C.R., Peterson, J.R., Kabukcu, C., Chapot, M.S., Melia, F., Rots, V., George, N., 2023. Evidence for the earliest structural use of wood at least 476,000 years ago. *Nature* 1–5.
- Callahan, E., 1979. The basics of bifacial knapping in the eastern fluted point tradition. *Archaeol. East. N. Am.* 7, 1–180.
- Caruana, M.V., 2020. South African handaxes reloaded. *J. Archaeol. Sci. Rep.* 34, 102649.
- Caruana, M.V., 2021. Pilot study comparing the effects of thinning processes on the cross-sectional morphologies of Early and Late Acheulian handaxes. *Archaeometry* 63, 481–499.
- Caruana, M.V., 2022. Extrapolating Later Acheulian handaxe reduction sequences in South Africa: a case study from the Cave of Hearths and Amanzi Springs. *Lithic Technol.* 47, 1–12.
- Caruana, M.V., Herries, A.I., 2020. An Acheulian balancing act: A multivariate examination of size and shape in Handaxes from Amanzi Springs, Eastern Cape, South Africa. In: Cole, J., McNabb, J., Grove, M., Hosfield, R. (Eds.), *Landscapes of Human Evolution*. Achaeopress, Oxford, U.K, pp. 91–115.
- Caruana, M.V., Herries, A.I., 2021. Modelling production mishaps in later Acheulian handaxes from the Area 1 excavation at Amanzi Springs (Eastern Cape, South Africa) and their effects on reduction and morphology. *J. Archaeol. Sci. Rep.* 39, 103121.
- Caruana, M.V., Wilson, C.G., Blackwood, A.F., Herries, A.I., 2022. Mitigating Mishaps: Diachronic Trends in Handaxe Shaping and Knapping Error Management at Amanzi Springs Area 2 (Eastern Cape, South Africa). *Lithic Technol.* 1–17.
- Caruana, M.V., Wilson, C.G., Arnold, L.J., Blackwood, A.F., Demuro, M., Herries, A.I., 2023. A marine isotope stage 13 Acheulian sequence from the Amanzi Springs Area 2 Deep Sounding excavation, Eastern Cape, South Africa. *J. Hum. Evol.* 176, 103324.
- Clarkson, C., 2013. Measuring core reduction using 3D flake scar density: a test case of changing core reduction at Klasies River Mouth, South Africa. *J. Archaeol. Sci.* 40, 4348–4357.
- Crompton, R.H., Gowlett, J.A., 1993. Allometry and multidimensional form in Acheulean bifaces from Kilombe, Kenya. *J. Hum. Evol.* 25, 175–199.
- de la Torre, I., Mora, R., Arroyo, A., Benito-Calvo, A., 2014. Acheulean technological behaviour in the middle Pleistocene landscape of Mieso (East-Central Ethiopia). *J. Hum. Evol.* 76, 1–25.
- de la Torre, I., Mora, R., 2018. Technological behaviour in the early Acheulean of EF-HR (Olduvai Gorge, Tanzania). *J. Hum. Evol.* 120, 329–377.
- Deacon, H.J., 1970. The Acheulian Occupation at Amanzi Springs, Uitenhage District, Cape Province. In: *Annals of the Cape Province Museum*, 8. South Africa, Grahamstown.
- Duller, G.A., Tooth, S., Barham, L., Tsukamoto, S., 2015. New investigations at Kalambo Falls, Zambia: Luminescence chronology, site formation, and archaeological significance. *J. Hum. Evol.* 85, 111–125.
- Gallotti, R., Mussi, M., 2017. Two Acheuleans, two humankinds: From 1.5 to 0.85 ma at Melka Kunture (upper awash, Ethiopian highlands). *J. Anthropol. Sci.* 95, 1–46.
- Gallotti, R., Raynal, J.P., Geraads, D., Mussi, M., 2014. Garba XIII (Melka Kunture, Upper Awash, Ethiopia): A new Acheulean site of the late Lower Pleistocene. *Quat. Int.* 343, 17–27.
- Gallotti, R., Muttoni, G., Lefèvre, D., Degeai, J.P., Geraads, D., Zerboni, A., Andrieu-Ponel, V., Maron, M., Perini, S., El Graoui, M., Sanz-Laliberté, S., 2021. First high resolution chronostratigraphy for the early North African Acheulean at Casablanca (Morocco). *Sci. Rep.* 11, 15340.
- Gallotti, R., Raynal, J.P., Mohib, A., Fernandes, P., Magoga, L., El Graoui, M., Rué, M., Muttoni, G., Lefèvre, D., 2023. Early North African Acheulean techno-economic systems at Thomas Quarry I-L1 (Casablanca, Morocco). *J. Anthropol. Sci.* 101, 1–59.
- García-Medrano, P., Ashton, N., Moncel, M.H., Ollé, A., 2020. The WEAP method: A new age in the analysis of the Acheulean Handaxes. *J. Paleol. Archaeol.* 3, 756–793.
- Goren-Inbar, N., Saragusti, I., 1996. An Acheulian biface assemblage from Gesher Benot Ya'aqov, Israel: indications of African affinities. *J. Field Archaeol.* 23, 15–30.
- Goren-Inbar, N., Grosman, L., Sharon, G., 2011. The technology and significance of the Acheulian giant cores of Gesher Benot Ya'aqov Israel. *J. Archaeol. Sci.* 38, 1901–1917.
- Goren-Inbar, N., Alpers-Afil, N., Sharon, G., Herzlinger, G., 2018. The Acheulian site of Gesher Benot Ya'aqov volume IV: The lithic assemblages. Springer.
- Gowlett, J.A.J., 2006. The Elements of Design Form in Acheulian Bifaces: Modes, Modalities, Rules and Language. In: Goren-Inbar, N., Sharon, G. (Eds.), *Axe Age: Acheulian Toolmaking from Quarry to Discard*. Equinox, London, pp. 203–221.
- Hallós, J., 2005. "15 Minutes of Fame": exploring the temporal dimension of Middle Pleistocene lithic technology. *J. Hum. Evol.* 49, 155–179.
- Herries, A.I., Arnold, L.J., Boschian, G., Blackwood, A.F., Wilson, C., Mallett, T., Armstrong, B., Demuro, M., Petchev, F., Meredith-Williams, M., Penzo-Kajewski, P., 2022. A marine isotope stage 11 coastal Acheulian workshop with associated wood at Amanzi Springs Area 1. South Africa. *Plos One* 17, e0273714.
- Herzlinger, G., Goren-Inbar, N., 2019. Do a few tools necessarily mean a few people? A techno-morphological approach to the question of group size at Gesher Benot Ya'aqov Israel. *J. Hum. Evol.* 128, 45–58.
- Herzlinger, G., Goren-Inbar, N., 2020. Beyond a cutting edge: A morpho-technological analysis of Acheulian handaxes and cleavers from Gesher Benot Ya'aqov Israel. *J. Paleol. Archaeol.* 3, 33–58.
- Herzlinger, G., Goren-Inbar, N., Grosman, L., 2017a. A new method for 3D geometric morphometric shape analysis: The case study of handaxe knapping skill. *J. Archaeol. Sci. Rep.* 14, 163–173.
- Herzlinger, G., Grosman, L., 2018. AGMT3-D: A software for 3-D landmarks-based geometric morphometric shape analysis of archaeological artifacts. *PLoS One* 13, e0207890.
- Herzlinger, G., Wynn, T., Goren-Inbar, N., 2017b. Expert cognition in the production sequence of Acheulian cleavers at Gesher Benot Ya'aqov, Israel: A lithic and cognitive analysis. *PLoS One* 12, e0188337.
- Inskeep, R., 1965. Earlier Stone Age Occupation at Amanzi: Preliminary Investigations. *S. Afr. J. Sci.* 61, 229–242.
- Isaac, G.L., Keller, C.M., 1968. Note on the proportional frequency of side-and end-struck flakes. *The South African Archaeological Bulletin.* 23, 17–19.
- Jones, P.R., 1994. Results of experimental work in relation to the stone industries of Olduvai Gorge. In: Leakey, M.D., Roe, D.A. (Eds.), *Olduvai Gorge: Excavations in Beds III. IV and the Masek Beds*, Cambridge University Press, Cambridge, pp. 1968–1971.
- Keller, C.M., 1973. *Montagu Cave in Prehistory: A Descriptive Analysis*. Anthropological Records 28, 1–98.
- Leader, G.M., 2014. New excavations at Canteen Kopje, Northern Cape Province, South Africa: a techno-typological comparison of three earlier Acheulean assemblages with new interpretations on the Victoria West phenomenon. University of the Witwatersrand. Unpublished PhD thesis. Johannesburg.
- Li, H., Kuman, K., Lotter, M.G., Leader, G.M., Gibbon, R.J., 2017. The Victoria West: earliest prepared core technology in the Acheulean at Canteen Kopje and implications for the cognitive evolution of early hominids. *R. Soc. Open Sci.* 4, 170288.
- Madsen, B., Goren-Inbar, N., 2004. Acheulian giant core technology and beyond: an archaeological and experimental case study. *Eurasian Prehistory.* 2, 3–52.
- McBrearty, S., 2001. The Middle Pleistocene of East Africa. In: Barham, L.S., Robson-Brown, K. (Eds.), *Human Roots: Africa and Asia in the Middle Pleistocene*. Western Academic & Specialist Press Ltd, U.K, Bristol, pp. 81–97.
- McNabb, J., 2009. The ESA stone tool assemblage from the Cave of Hearths, Beds 1–3. In: McNabb, J., Sinclair, A. (Eds.), *The Cave of Hearth Makapan Pleistocene Research Project: Field Research by Anthony Sinclair and Patrick Quinney, 1996–2001*. Achaeopress, Oxford, U.K., pp. 75–104.

- McNabb, J., Beaumont, P., 2011. Excavations in the Acheulean levels at the Earlier Stone Age site of Canteen Koppie, Northern Province, South Africa. In: *Proceedings of the Prehistoric Society*, 78, Cambridge University Press., Cambridge, pp. 51-71.
- McNabb, J., Binyon, F., Hazelwood, L., 2004. The large cutting tools from the South African Acheulean and the question of social traditions. *Curr. Anthropol.* 45, 653-677.
- Muir, R.A., Bordy, E.M., Reddering, J.S.V., Viljoen, J.H.A., 2017. Lithostratigraphy of the Enon Formation (Uitenhage Group), South Africa. *S. Afr. J. Geol.* 2017 (120), 273-280.
- Newcomer, M.H., 1971. Some quantitative experiments in handaxe manufacture. *World Archaeol.* 3, 85-94.
- Newcomer, M.H., Hivernel-Guerre, F., 1974. Nucléus sur éclat: technologie et utilisation par différentes cultures préhistoriques. *Bulletin de la Société préhistorique française. Comptes rendus des séances mensuelles*, 119-128.
- Owen, W.E., 1938. The Kombewa culture, Kenya Colony. *Man* 38, 203-205.
- Paddayya, K., 1977. The Acheulian Culture of the Hunsgi Valley (Shorapur Doab), Peninsular India. *Proc. Am. Philos. Soc.* 121, 383-406.
- Paddayya, K., 1982. The Acheulian Culture of the Hunsgi Valley (Peninsular India): A Settlement System Perspective. Deccan College, Pune.
- Paddayya, K., Blackwell, B.A., Jhaladiyal, R., Petraglia, M.D., Fevrier, S., Chaderton, D.A., Blickstein, J.I., Skinner, A.R., 2002. Recent findings on the Acheulian of the Hunsgi and Baichbal valleys, Karnataka, with special reference to the Isampur excavation and its dating. *Curr. Sci.* 641-647.
- Paddayya, K., Jhaladiyal, R., Petraglia, M.D., 2006. The acheulian quarry at Isampur, lower Deccan, India. In: Goren-Inbar, N., Sharon, G. (Eds.), *Axe Age: Acheulian Toolmaking from Quarry to Discard*. Equinox, London, pp. 45-73.
- Petraglia, M., LaPorta, P., Paddayya, K., 1999. The first Acheulian quarry in India: stone tool manufacture, biface morphology, and behaviors. *J. Anthropol. Res.* 55, 39-70.
- Petraglia, M.D., Shipton, C., Paddayya, K., 2005. Life and mind in the Acheulean: a case study from India. In: Gamble, C., Porr, M. (Eds.), *Hominid Individual in Context*. Routledge, pp. 214-236.
- Potts, R., Behrensmeier, A.K., Ditchfield, P., 1999. Paleolandscape variation and Early Pleistocene hominid activities: members 1 and 7, Olorgesailie Formation Kenya. *J. Hum. Evol.* 37, 747-788.
- Presnyakova, D., Braun, D.R., Conard, N.J., Feibel, C., Harris, J.W., Pop, C.M., Schlager, S., Archer, W., 2018. Site fragmentation, hominin mobility and LCT variability reflected in the early Acheulean record of the Okote Member, at Koobi Fora Kenya. *J. Hum. Evol.* 125, 159-180.
- Preysler, J.B., Navas, C.T., Sharon, G., 2018. Life history of a large flake biface. *Quat. Sci. Rev.* 190, 123-136.
- R Core Team. (2013). R: A Language and Environment for Statistical Computing. Foundation for Statistical Computing. <http://www.r-project.org/index.htm>.
- Roe, D.A., 1968. British Lower and Middle Palaeolithic Handaxe Groups. *Proceedings of the Prehistoric Society*, 34, 1-82.
- Santónja, M., Rubio-Jara, S., Panera, J., Pérez-González, A., Rojas-Mendoza, R., Domínguez-Rodrigo, M., Mabulla, A.Z. and Baquedano, E., 2018. Bifacial shaping at the TK Acheulean site (Bed II, Olduvai Gorge, Tanzania): new excavations 50 years after Mary Leakey. In: Galloti, R., Mussi, M., (Eds.), *The Emergence of the Acheulean in East Africa and Beyond: Contributions in Honor of Jean Chavaillon*, pp.153-181.
- Schick, K., Clark, J.D., 2003. Biface technological development and variability in the Acheulean industrial complex in the Middle Awash region of the Afar Rift, Ethiopia. In: Soressi, M., Dibble, H.L. (Eds.), *Multiple Approaches to the Study of Bifacial Technologies*. University of Pennsylvania, Philadelphia, pp. 1-30.
- Sharon, G., 2007. Acheulian large flake industries: technology, chronology, and significance. *BAR International Series*, Oxford, U.K.
- Sharon, G., 2008. The impact of raw material on Acheulian large flake production. *J. Archaeol. Sci.* 35, 1329-1344.
- Sharon, G., 2009. Acheulian giant-core technology: a worldwide perspective. *Curr. Anthropol.* 50, 335-367.
- Sharon, G., 2010. Large flake acheulian. *Quat. Int.* 223, 226-233.
- Sharon, G., 2011. Flakes crossing the straits? Entame flakes and northern Africa-Iberia contact during the Acheulean. *Afr. Archaeol. Rev.* 28, 125-140.
- Sharon, G., 2019. Early Convergent Cultural Evolution: Acheulean Giant Core Methods of Africa. In: Overmann, K.A., Coolidge, F.L. (Eds.), *Squeezing Minds from Stones: Cognitive Archaeology and the Evolution of the Human Mind*. Oxford University Press, Oxford, pp. 237-250.
- Sharon, G., Beaumont, P., 2006. Victoria West: a highly standardized prepared core technology. In: Goren-Inbar, N., Sharon, G. (Eds.), *Axe Age: Acheulian Toolmaking from Quarry to Discard*. Equinox, London, pp. 181-200.
- Sharon, G., Alpers-Afil, N., Goren-Inbar, N., 2011. Cultural conservatism and variability in the Acheulean sequence of Gesher Benot Ya 'aqov. *J. Hum. Evol.* 60, 387-397.
- Shelley, P.H., 1990. Variation in lithic assemblages: An experiment. *J. Field Archaeol.* 17, 187-193.
- Shipton, C., 2011. Taphonomy and behaviour at the Acheulean site of Kariandusi Kenya. *Afr. Archaeol. Rev.* 28, 141-155.
- Shipton, C., 2018. Biface knapping skill in the East African Acheulean: Progressive trends and random walks. *Afr. Archaeol. Rev.* 35, 107-131.
- Shipton, C., 2022. Predetermined refinement: The earliest Levallois of the Kapthurin formation. *J. Palaeol. Archaeol.* 54, 1-29.
- Shipton, C., Clarkson, C., 2015. Flake scar density and handaxe reduction intensity. *J. Archaeol. Sci. Rep.* 2, 169-175.
- Shipton, C., Parton, A., Breeze, P., Jennings, R.P., Groucutt, H.S., White, T.S., Drake, N., Crassard, R., Alsharekh, A., Petraglia, M.D., 2014. Large flake Acheulean in the Nefud Desert of northern Arabia. *PaleoAnthropology* 2014, 446-462.
- Shipton, C.B.K., Petraglia, M.D., Paddayya, K., 2009. Stone tool experiments and reduction methods at the Acheulean site of Isampur Quarry, India. *Antiquity* 83, 769-785.
- Stout, D., Apel, J., Commander, J., Roberts, M., 2014. Late Acheulean technology and cognition at Boxgrove UK. *J. Archaeol. Sci.* 41, 576-590.
- Texier, P.J., Roche, H., 1995. The impact of predetermination on the development of some Acheulean chaînes opératoires. In: Bermúdez de Castro, J., Arsuaga, J.L., Carbonell, E. (Eds.), *Evolución Humana En Europa y Los Yacimientos De La Sierra De Atapuerca*. Junta de Castilla y Leon, Valladolid., pp. 403-420.
- Tixier, J., 1956. Le hachereau dans l'Acheuléen nord-africain. *Notes typologiques. s. In: Congrès préhistorique de France - Compte-rendu de la XVème session - Poitiers Angoulême - 15-22 juillet 1956, Congrès préhistorique de France*, pp. 914-923.
- Toth, N., 2001. Experiments in quarrying large flake blanks at Kalambo Falls. In: J.D. Clark (Eds.), *Kalambo Falls prehistoric site, Vol. III*, Cambridge University Press, Cambridge., pp. 600-604.
- Tryon, C.A., McBrearty, S., Texier, P.J., 2005. Levallois lithic technology from the Kapthurin formation, Kenya: Acheulian origin and Middle Stone Age diversity. *Afr. Archaeol. Rev.* 22, 199-229.
- Whittaker, J.C., 1994. *Flintknapping: Making and Understanding Stone Tools*. University of Texas Press.
- Winton, V., 2005. An investigation of knapping-skill development in the manufacture of Palaeolithic handaxes. In: Roux, V., Bril, B. (Eds.), *Stone Knapping: the Necessary Conditions for a Uniquely Hominin Behaviour*. McDonald Institute for Archaeological Research, Cambridge, U.K., pp. 109-116.
- Wynn, T., Gowlett, J., 2018. The handaxe reconsidered. *Evolution. Anthropol. Issues, News Rev.* 27, 21-29.